Well-Defined Amphiphilic Thermosensitive Copolymers Based on Poly(ethylene glycol monomethacrylate) and Methyl Methacrylate Prepared by Atom Transfer Radical Polymerization

Mir Mukkaram Ali and Harald D. H. Stöver*

Department of Chemistry, McMaster University, 1280 Main Street West, Hamilton, Ontario L8S 4M1, Canada

Received September 17, 2003; Revised Manuscript Received January 18, 2004

ABSTRACT: Amphiphilic homopolymers of the hydroxy-functional macromonomer poly(ethylene glycol) monomethacrylate (PEGMA) and its copolymers with methyl methacrylate (MMA) were prepared by atom transfer radical polymerization. Commercially available PEGMA (Aldrich) contains nonfunctional poly(ethylene glycol) (PEG), monofunctional PEGMA, and difunctional poly(ethylene glycol) dimethacrylate (PEGDMA) in a 1:3:1 ratio as analyzed by HPLC. A solvent extraction procedure yielded a PEGMA enriched mixture (PEG:PEG-MA:PEGDMA = 5:92:3) with PEGMA M_n values of 480 and 410 Da based on HPLC and ^{1}H NMR, respectively. ATRP homopolymerization of this purified PEGMA in the hydroxyl-bearing solvents, cyclohexanol and ethanol (ϵ = 16.4 and 25.3, respectively), yielded well-defined homopolymers (M_w/M_n < 1.1). On the other hand, ATRP copolymerizations with MMA (PEGMA content = 10, 18, 24, 30, and 40 mol %) yielded best results in non-hydrogen-bonding diphenyl ether (ϵ = 3.37). The homopolymer and copolymers containing more than 24 mol % (57 wt %) PEGMA were water-soluble and exhibited sharp lower critical solution temperatures (LCST) that increased with increasing PEGMA content as expected. Unlike similar PEGMA-based amphiphilic copolymers prepared by conventional free radical polymerizations, the ATR polymerizations reported here proceeded to high conversions (60−100%) and yielded well-defined polymers (M_w/M_n = 1.1−1.15) with no gel fraction that remained linear and water-soluble after storage in ambient conditions for several months.

Introduction

Atom transfer radical polymerization (ATRP) is a recent living/controlled radical polymerization method[1,2] which has been developed extensively owing to its tolerance of a wide range of functional groups and to the relatively nonstringent experimental conditions required for this polymerization.[3,4] In ATRP radicals are formed by a redox transfer of a halide atom from a initiator halide to a transition-metal-based catalyst. The formed radicals add monomer and react with the oxidized metal catalyst to re-form a halogen-capped dormant species. The resulting active radical/dormant species equilibrium lies predominantly on the side of the dormant species, thereby maintaining a very low equilibrium radical concentration, which minimizes chain termination. Furthermore, a fast dynamic equilibrium between the active radical and halide-capped dormant species ensures that all growing chains get an equal opportunity to add monomer units, resulting in low-polydispersity polymer. While ATRP is usually employed for the preparation of well-defined polymers and block copolymers, immobilizing ATRP initiators on substrates allows growth of polymer chains from surfaces via the "grafting from" approach, thereby imparting desirable properties to the substrate. Immobilization of conventional free radical polymerization initiators yields high graft densities but results in poor control of molecular weight and polydispersity.[5,6] ATRP grafting offers better control over these properties[7−9] and enables block copolymer grafting.[10]

One particularly interesting class of polymers to be grafted from surfaces are thermally responsive polymers (TRP's). The development of ATRP to form novel TRPs in solution conditions is a necessary precursor for a myriad of potential surface grafting applications and is the subject of this work. TRPs have been the subject of intensive research in recent years[11] due to their potential in diverse areas such as controlled drug delivery,[12,13] reversible surfactants,[14,15] chromatography,[16] and the development of new methods of fighting microbial and other biofouling of surfaces.[17] Temperature-induced swelling and shrinking of drug-loaded TRP macrogels may be used to absorb/release drugs.[18] Similarly, release from microcapsules may be thermally modulated either by surface coating the capsule[19] or by filling the cavities in the capsule with TRPs.[20] As well, surface grafting of TRP's on porous membranes using living polymerization techniques has been explored.[21]

Brush-shaped copolymers based on poly(ethylene glycol) monomethyl ether methacrylates exhibiting soft elastomeric properties have recently been prepared by ATRP.[22,23] Also, similar methoxy-capped oligoethylene glycol methacrylates were polymerized by living anionic polymerization, yielding well-defined thermoresponsive comb-shaped polymers.[24] However, well-defined hydroxyl-bearing oligoethylene glycol analogues have only been prepared via ionic polymerization of hydroxyl-protected monomers.[25]

We report the solution atom transfer radical homopolymerization of hydroxyl-bearing poly(ethylene glycol monomethacrylate) and its copolymerization with methyl methacrylate in organic solvents, using toluenesulfonyl chloride as initiator and Cu(I)Br/alkylbipyridine as catalyst. The polymerizations yielded narrow disperse polymers (M_w/M_n < 1.15) with molecular weights reflecting the monomer-to-initiator ratio. Unlike conventional free radical polymerizations of PEGMA which yield cross-linked gels in the absence of added chain transfer agents and typically cross-link during storage,[26]

* Corresponding author. E-mail stoverh@mcmaster.ca.

10.1021/ma030485m CCC: $27.50
Published on Web 06/09/2004

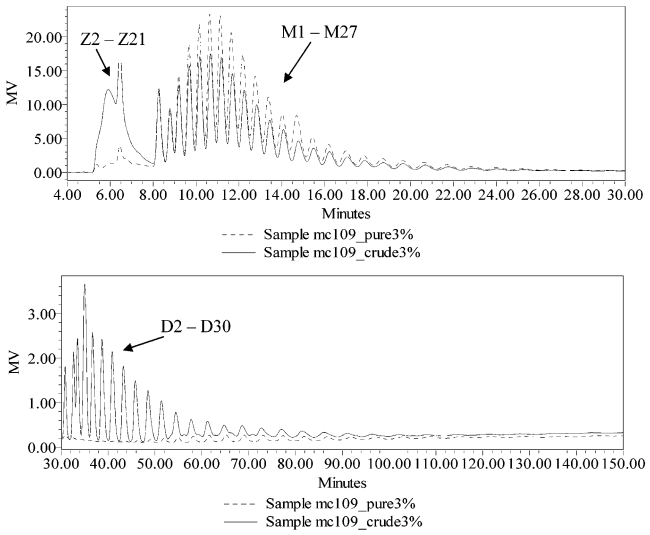

Figure 1. Overlaid HPLC chromatograms of crude (solid line) and purified (dotted line) poly(ethylene glycol) monomethacrylate (Aldrich). Chromatographic conditions as follows: reverse phase C-18 column; mobile phase: methanol/water = 1:1; flow rate = 0.5 mL/min; column temperature = 35 °C; refractive index detector temperature = 30 °C; sample concentration = 3 wt %; injection volume = 20 μL; run time = 150 min. Nonfunctional PEG components (Z2−Z21) elute in the 5−8 min retention time range; monofunctional PEG-MA components (M1−M27) elute in the 8−30 min range; and difunctional PEG-DMA (D2−D30) elute in the 30−150 min range.

the ATRP products remained linear and soluble over several months of storage. The homopolymer and copolymers containing more than 57 mol % PEGMA are water-soluble. The water-soluble copolymers exhibit lower critical solution temperatures that could be varied with the comonomer ratio. This work has potential for the development of smart materials based on substrates bearing surface grafted thermoresponsive polymer.

Results and Discussion

HPLC Analysis of PEGMA Macromonomer. PEGMA is commercially available from Aldrich and Polysciences, Inc., and is quoted as having a M_n of 360 and 285 Da (n = 200; where "n" is the molecular weight of the pendant poly(ethylene glycol) chain), respectively. As PEGMA is commonly prepared by methacrylate functionalization of poly(ethylene glycol) (PEG), we anticipated that the macromonomer would be comprised of the nonfunctional PEG, monofunctional poly(ethylene glycol) monomethacrylate (PEG-MA), and difunctional, poly(ethylene glycol) dimethacrylate (PEG-DMA). This is in contrast to poly(ethylene glycol) monomethyl ether methacrylate (MPEGMA), which is prepared by reaction of PEG oligomers (bearing a nonreactive methoxy terminus on one end and a reactive hydroxyl group on the other) with methacryloyl chloride in a quantitative reaction and hence only contains the monofunctional homologues.[27] PEGMA was analyzed using a reverse phase C-18 HPLC column and methanol:water (1:1) as mobile phase. The peaks in the overlaid chromatograms (Figure 1) were analyzed by LC-MS, and those in the 5−8 min retention time region were assigned to zero-functional PEG containing 2−21 ethylene oxide units (Z2−Z21), 8−30 min range to monofunctional PEG-MA containing 1−27 ethylene oxide units (M1−M27), and 30−150 min range to difunctional PEG-DMA containing 2−30 ethylene oxide units (D2−D30). The mass spectral data are presented in Table 1.

Table 1. LC-MS Data for Crude PEGMA

n	monofunc FW	compds M+1[a]	difunc FW[b]	compds M+1[a]	nonfunc FW[b]	compds M+1[a]
1	130.14	**131.14**	*198.21*	199.21	*62.07*	63.07
2	174.19	**175.19**	242.26	**243.26**	106.12	**107.12**
3	218.24	**219.24**	286.31	**287.31**	150.17	**151.17**
4	262.29	**263.29**	330.36	**331.36**	194.22	**195.22**
5	306.34	**307.34**	374.41	**375.41**	238.27	**239.27**
6	350.39	**351.39**	418.46	**419.46**	282.32	**283.32**
7	394.44	**395.44**	462.51	**463.51**	326.37	**327.37**
8	438.49	**439.49**	506.56	**507.56**	370.42	**371.42**
9	482.54	**483.54**	550.61	**551.61**	414.47	**415.47**
10	526.59	**527.59**	594.66	**595.66**	458.52	**459.52**
11	570.64	**571.64**	638.71	**639.71**	502.57	**503.57**
12	614.69	**615.69**	682.76	**683.76**	546.62	**547.62**
13	658.74	**659.74**	726.81	**727.81**	590.67	**591.67**
14	702.79	**703.79**	770.86	**771.86**	634.72	**635.72**
15	746.84	**747.84**	814.91	**815.91**	678.77	**679.77**
16	790.89	**791.89**	858.96	**859.96**	722.82	**723.82**
17	834.94	**835.94**	903.01	904.01	766.87	**767.87**
18	878.99	**879.99**	947.06	948.06	810.92	**811.92**
19	923.04	**924.04**	991.11	992.11	854.97	**855.97**
20	967.09	**968.09**	1035.16	1036.16	899.02	**900.02**
21	1011.14	1012.14	1079.21	1080.21	943.07	**944.07**
22	1055.19	1056.19	1123.26	1124.26		
23	1099.24	1100.24	1167.31	1168.31		
24	1143.29	1144.29	1211.36	1212.36		
25	1187.34	1188.34	1255.41	1256.41		
26	1231.39	1232.39	1299.46	1300.46		
27	1275.44	1276.44	1343.51	1344.51		
28			1387.56	1388.56		
29			1431.61	1432.61		
30			1475.66	1476.66		

[a] Components shown in bold were detected in the mass spectrum while the others were assigned by extrapolation. [b] Components in italics are not present in the LC-MS but have been retained here for reference.

Table 2. Refractive Indices of Some Oligo Ethylene Glycols and Dimethacrylate Derivatives

compound	refractive index (Aldrich)
ethylene glycol	1.431
diethylene glycol	1.446
triethylene glycol	1.455
poly(ethylene glycol)	1.454
ethylene glycol dimethacrylate	1.454
diethylene glycol dimethacrylate	1.458
triethylene glycol dimethacrylate	1.46
poly(ethylene glycol) dimethacrylate (M_n = 330 Da)	1.463

The chromatograms in Figure 1 were acquired using a refractive index detector. Since the refractive indexes of the zero, monofunctional, and difunctional homologues are similar (Table 2), the areas under the peaks were used to quantitatively determine the composition of PEGMA. This indicated that the composition of crude PEGMA is PEG:PEG-MA:PEG-DMA = 19:60:21 and yielded a number-average molecular weight (M_n) of 453 Da for monofunctional components and 466 Da for the mixture of mono- and difunctional components. The M_n assigned by the supplier (∼360 Da) therefore significantly differs from the averaged values obtained here from HPLC.

Isolation and Analysis of Monofunctional PEG-MA. PEG-MA was isolated from the mixture by extraction of its aqueous solution with diphenyl ether (DPE) to selectively remove the PEG-DMA followed by an extraction of the resulting aqueous phase with a 3:1 mixture of methylene chloride and hexanes (CH_2Cl_2/C_6H_{14})[28] to partition the PEG-MA almost entirely into the organic phase from which it was recovered by

Table 3. Dielectric Constants and Solubility Parameters of Some ATRP Solvents

solvent	solubility parameter[a]/MPa$^{1/2}$	dielectric constant (ϵ)[b] (T/K)
p-xylene	18	2.27 (293.2)
diphenyl ether	20.9	3.73 (283.2)
n-butyl acetate	17.4	5.07 (293.2)
cyclohexanol	22.5	16.4 (293.2)
ethanol	26.6	25.3 (293.2)

[a] Source: Grulke, E. A. In Solubility Parameter values. *Polymer Handbook*, 4th ed.; John Wiley and Sons: New York, 1999; Table 7, p VII/688. [b] Source: Wohlfarth, C. In *CRC Handbook of Chemistry and Physics*, 76th ed.; CRC Press: Boca Raton, FL, 1995−1996; p 6-159.

solvent evaporation. Integration of the area under the peaks in the chromatograms of crude and purified PEGMA (Figure 1) showed that purified PEGMA is composed of PEG:PEG-MA:PEG-DMA = 5:92:3 (19:60:21 in crude PEGMA). The area under the component peaks was also used to calculate the number-average molecular weight of purified PEGMA and yielded an M_n of 480 Da for monofunctional components and 510 Da for the mixture of mono- and difunctional components. The M_n values were further verified by ^{1}H NMR. The ratio of the peak areas of the vinyl protons (δ_H = 6.1 and 5.6 ppm) to that of the methylene protons in the pendant PEG chain (δ_H = 4.3 and 3.6 ppm) in the ^{1}H NMR spectrum of purified PEGMA indicated an average of 7.3 ethylene oxide units in the pendant PEG chain or a formal M_n of 410 Da.

ATRP Synthesis of Poly(poly(ethylene glycol) monomethacrylate) (P(PEGMA)). Good control over polymer molecular weight and polydispersity in ATRP depends on fast initiation relative to propagation, a low radical concentration, and a fast dynamic equilibrium between the active and dormant radicals. In general, arenesulfonyl halides in conjunction with Cu(I) halide/bipyridine catalysts serve as efficient ATRP initiators for methacrylates,[29] with initiation rates being 4 orders of magnitude higher than the propagation rate and near 100% initiation efficiency. We have previously demonstrated the efficacy of this system for the copolymerization of MMA with poly(ethylene glycol) monomethyl ether methacrylate (MPEGMA).[27]

Thus, toluenesulfonyl chloride (TSC) was used as the ATRP initiator with a catalyst based on copper(I) bromide and 4,4′-dinonyl-2,2′-dipyridyl. The solvent polarity can significantly affect the position of the active radical−dormant species equilibrium and is therefore a key parameter in determining the success of an ATRP reaction.[30−32] Accordingly, we studied the ATR homopolymerization of PEGMA in a series of organic solvents of varying polarity and hydrogen-bonding characteristics (Table 3). Bo et al.[26] studied the conventional free radical copolymerization of PEGMA ($M_n \sim$ 400 Da) with MMA and ethylhexyl acrylate and reported that the formation of cross-linked gels could be avoided only by conducting the polymerizations below 30% monomer loading and in the presence of chain transfer agents. Cross-linking was attributed to chain transfer to polymer. In view of Bo's report, we conducted all homopolymerizations and copolymerizations at 25 wt % monomer loading. We believe the cross-linking observed by Bo et. al. was in part due to chain transfer to pendant PEG moieties as concluded by the authors but may also have been due to significant quantities of difunctional cross-linking monomer present in their polymerizations.

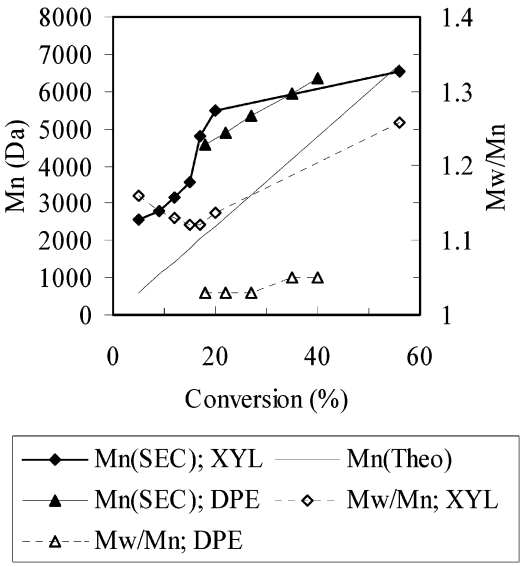

Figure 2. Molecular weight and polydispersity profiles for polymerization of PegMA in DPE and XYL at 25 wt % monomer loading. $[TSC]_0$:$[Cu(dNBpy)_2Br]_0$:[PEGMA] = 1:1:30 at 70 °C.

Diphenyl ether (DPE) and xylene (XYL) provide a pair of aprotic solvents that differ significantly in their overall polarity (solubility parameters, δ_{XYL} = 18.0 MPa$^{1/2}$ and δ_{DPE} = 20.9 MPa$^{1/2}$; dielectric constants, ϵ_{XYL} = 2.27; ϵ_{DPE} = 3.73). Furthermore, we have previously shown that DPE and XYL are good solvents for ATRP of methyl methacrylate.[33] Hence, the ATRP homopolymerization of PEGMA was first attempted in these two solvents. Both MMA and PEGMA are methacrylates, but with three key differences. First, PEGMA, being a macromonomer, suffers from having a low concentration of polymerizable groups in the system plus possible steric hindrance during the monomer addition as well as the atom transfer reactions with the catalyst. The former could lower the polymerization rate, and the latter could alter the position of active radical/dormant species equilibrium. Second, PEGMA is a more polar macromonomer than MMA and bears a hydroxyl group, both properties that are known to increase the activation rate constant in ATRP.[3,5] Third, PEGMA bears a pendant ether moiety that imparts it coordination ability. Haddleton et al.[34] observed an unusually high rate of polymerization of methoxy-terminated poly(ethylene glycol) methacrylate and attributed it to complexation of the oxyethylene groups to the copper in a dynamic competition with the alkyl-2-pyridylmethanimine ligand, resulting in a more active catalyst. Thus, although we have previously demonstrated that ATRP of MMA in DPE and XYL is successful, the PEGMA system may behave differently.

Figures 2 and 3 give the molecular weight and molecular weight distribution and the kinetic results for the ATRP results of PEGMA in DPE and XYL. In both polymerizations, the reaction mixture turned bright green upon initiator addition, indicating that TSC initiation is fast. However, we observed a significant difference in the post-initiation equilibrium concentration of Cu(I)/Cu(II) species in the polymerization medium, with green Cu(II) species being more predominant in the DPE case. This indicates that the deactivation rate constant in DPE is lower than that in XYL, possibly due to a change in the redox potential of the catalyst in more polar DPE (ϵ_{XYL} = 2.27 and ϵ_{DPE} = 3.73). In even

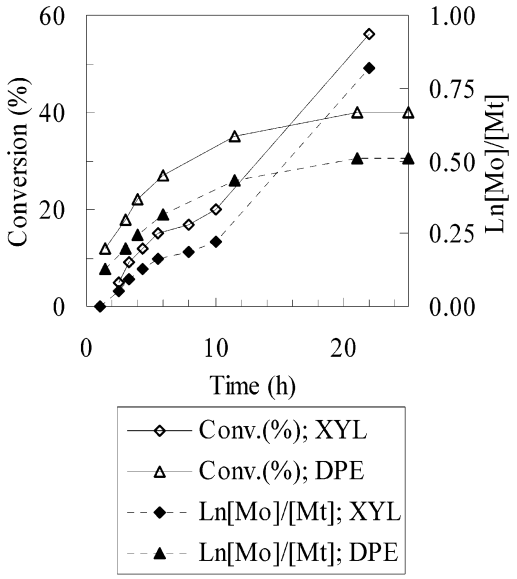

Figure 3. Conversion and kinetic profiles for polymerization of PegMA in DPE and XYL. Conditions as in Figure 2.

more polar butyl acetate ($\epsilon_{BuAc} = 5.07$), the polymerization mixture turned bright green upon initiation and remained bright green with no polymer forming after 24 h. We attribute this to a very low deactivation rate constant that leads to high radical concentration and consequent irreversible radical−radical termination as evidenced by the permanent green color of the reaction medium. Thus, we conclude that the deactivation rate constant is inversely related to the polarity of the reaction solvent. The lower deactivation rate constant in DPE leads to fast polymerization but low final conversion to polymer due to irreversible radical−radical termination as evidenced by the significant curvature in the kinetic plot (Figure 3). The molecular weight increased linearly with conversion after an initial exponential growth and prior to establishment of the Cu(I)/Cu(II) equilibrium (Figure 2). The conversion profile was as expected.

On the other hand, in XYL, molecular weight increased exponentially between 10 and about 30% conversion to polymer. This unusual behavior was accompanied by broadening polydispersity (Figure 2) and an unusual positive deviation in the kinetic and conversion profiles (Figure 3). The SEC chromatogram of the 22 h sample was bimodal, indicating that a significant amount of high molecular weight material formed in the latter part of the reaction. This high molecular weight polymer may result from coupling of methacrylate polymer radicals and radicals resulting from chain transfer to polymer, forming branched polymer with molecular weights 2−3 times higher than the peak average. While this explains the exponential increase in molecular weight, it contradicts the upward trends in the conversion and kinetic profiles because radical−radical coupling should lower radical concentrations and decrease polymerization rates. We propose that the forming PEGMA microphase separates in nonpolar xylene and that Cu(I)/Cu(II) catalyst species within these polymer-rich domains favors higher radical concentrations and faster polymerization rates causing the observed exponential increase in polymer molecular weight and broadening polydispersity. This is consistent with the higher rate of polymerization observed in a more polar solvent DPE.

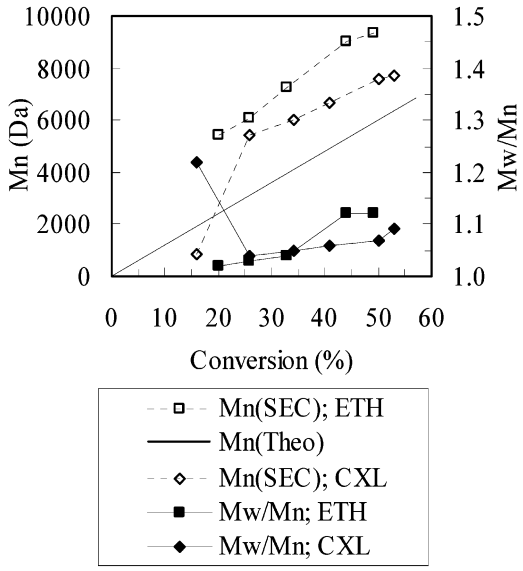

Figure 4. Molecular weight and polydispersity profiles for polymerization of PegMA in CXL and ETH at 25 wt % monomer loading. $[TSC]_0:[Cu(dNBpy)_2Br]_0:[PEGMA] = 1:1:30$ at 70 °C.

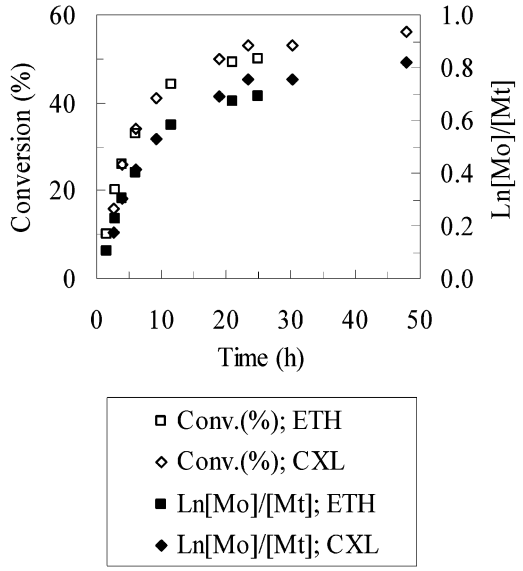

Figure 5. Conversion and kinetic profiles for polymerization of PegMA in CXL and ETH at 25 wt % monomer loading. $[TSC]_0:[Cu(dNBpy)_2Br]_0:[PEGMA] = 1:1:30$ at 70 °C.

Next, cyclohexanol (CXL) and ethanol (ETH) were chosen as a pair of strongly hydrogen bonding protic solvents that also differ in their overall polarity ($\delta_{CXL} = 22.5$ MPa$^{1/2}$, $\delta_{ETH} = 26.6$ MPa$^{1/2}$; $\epsilon_{CXL} = 16.4$; $\epsilon_{ETH} = 25.3$). In both solvents, the reaction mixture turned bright green upon initiation, and then gradually regained its deep red brown color in 1 and 2 h, respectively, indicating that the Cu(I) species predominates in the post-initiation Cu(I)/C(II) equilibrium. In both cases, the molecular weight increased nonlinearly up to ∼25 wt % conversion, beyond which point linear behavior was observed and the polydispersity remained low (Figure 4). Unlike the XYL system, in ETH and CXL, the conversion profile (Figure 5) exhibited the expected steady initial polymerization rate that leveled off at about 50 wt % final conversions to polymer. However, in both cases radical concentrations diminished significantly beyond 30% conversion as indicated by the curvature in kinetic profiles (Figure 5).

Table 4. Hydrophilic Lypophilic Balance of P(PEGMA) and P(PEGMA-*co*-MMA)

(co)polymer	mol % PEGMA	wt % PEGMA	HLB[a] (based on PEGMA content)	HLB[a] (based on PEG content)	water solubility (LCST/°C)
PEGMA-10	10	32	6.4	5	no
PEGMA-18	18	49	9.8	7.6	no
PEGMA-24	24	57	11.4	8.9	yes (42.7)
PEGMA-30	30	64	12.8	10	yes (49.8)
PEGMA-40	40	74	14.8	11.5	yes (55.8)
PEGMA-100[b]	100	100	20	15.6	yes (no)

[a] The hydrophilic lypophilic balance, HLB = (wt % of hydrophilic portion)/5. [b] PEGMA-100 is PEGMA homopolymer so its HLB based on PEGMA content is 20 by definition.

Since poly(ethylene glycol) monomethacrylate (PEGMA) is comprised of a mixture of monomers of varying PEG chain lengths, monomer incorporation into poly(poly(ethylene glycol) monomethacrylate) (P(PEGMA)) could be biased toward low molecular weight species. HPLC analysis of residual monomer showed that the homologue distribution in residual monomer is identical to that in the feed, indicating that monomer incorporation is independent of the macromonomer molecular weight.

ATRP Copolymerization of PEGMA and MMA. Amphiphilic copolymers exhibiting a range of hydrophilic lypophilic balance (HLB) were prepared by copolymerization of hydrophobic MMA with water-soluble PEGMA (Table 4). Since the ATRP of PEGMA was relatively successful in CXL, we anticipated that copolymerization with MMA might also be successful in this solvent. First, the homopolymerization of MMA in CXL was attempted prior to extending these solvent conditions to the copolymerization. In this experiment the forming PMMA phase separated in the solvent mixture, yielding a distinctly viscous polymer phase and a low-viscosity solvent phase. The polymerization however proceeded to quantitative conversion in this biphasic mixture. The product polymer was bimodal with 98% polymer exhibiting the theoretically expected molecular weight and low polydispersity (M_n = 8900 Da, M_w = 9400 Da, M_w/M_n = 1.06). The small amount (2%) of high molecular weight polymer (M_n = 65 000 Da, M_w = 83 000 Da, M_w/M_n = 1.28) could result from a Trommsdorff type effect in the viscous polymer phase.

Having proved that both MMA and PEGMA can be homopolymerized by ATRP in CXL, copolymers were prepared in this solvent and in DPE (a good solvent for ATRP copolymerization of methyl methacrylate and poly(ethylene glycol) monomethyl ether methacrylate).[27] The polymerization in CXL proceeded in a controlled manner as evidenced by the linear increase in molecular weight, and decrease in polydispersity, with conversion (Figure 6). The high polydispersity at reaction end (M_w/M_n = 1.5) could result from slow initiation (relative to propagation), from irreversible termination events during the polymerization or from a slow dynamic equilibrium between the active and dormant chains. Upon initiation, the polymerization mixture turned bright green and then turned back to a deep red-brown color, indicating fast initiation followed by establishment of the Cu(I)/Cu(II) equilibrium in which the Cu(I) species is predominant. Thus, slow initiation is unlikely to be the cause of the observed broad polydispersity. Also, the linearity of the kinetic plot (Figure 7) indicates no loss of radical concentration, suggesting that irreversible radical termination was insignificant. While slow dynamic equilibrium between the dormant and active polymer chains remains a plausible explanation, we believe the broad polydispersity is due to some uncontrolled polymerization in the early stages of the reaction. The SEC chromatograms of polymer at 27, 55, 77, and 99% conversion showed that the molecular weight of a minor (high molecular weight) peak in the bimodal distribution did not increase with conversion, indicating that these polymer chains were irreversibly terminated early in the reaction. This "dead" polymer was likely formed by uncontrolled polymerization prior to establishment of the required Cu(I)/Cu(II) equilibrium via the persistent radical effect and is responsible for the observed high polydispersity. The major peak (low molecular weight) peak shifted to higher molecular

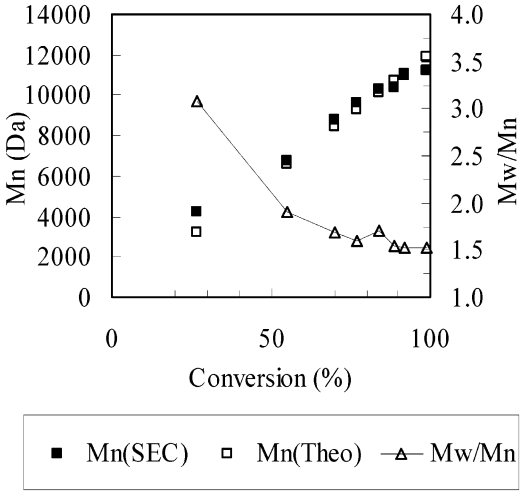

Figure 6. Molecular weight and polydispersity profiles for polymerization of P(MMA-*co*-PEGMA) (mol % PEGMA = 18) in CXL at 25 wt %. $[TSC]_0$:$[Cu(dNBpy)_2Br]_0$:[PEGMA] = 1:1:30 at 70 °C.

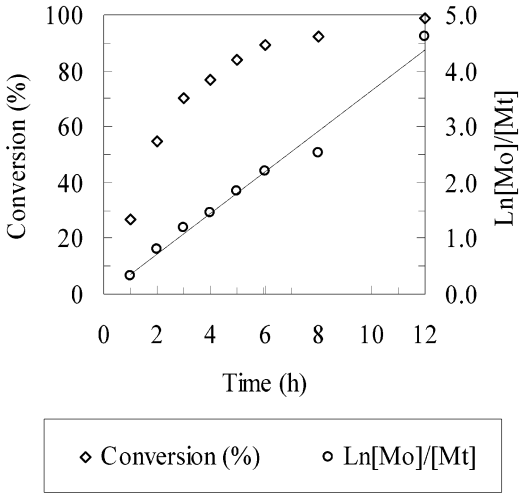

Figure 7. Conversion and kinetic profiles for polymerization of P(MMA-*co*-PEGMA) (mol % PEGMA = 18) in CXL. Conditions as in Figure 7.

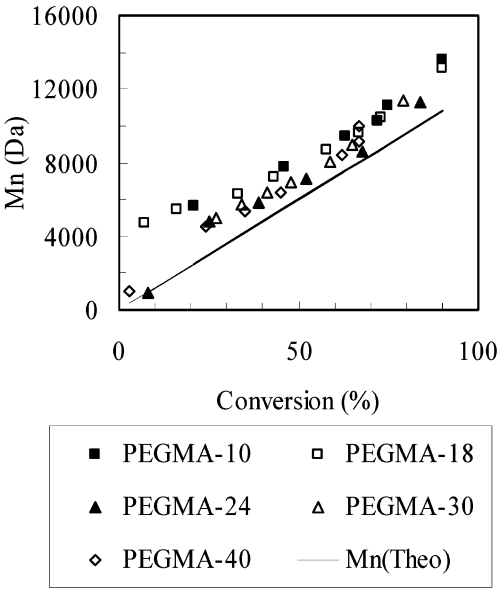

Figure 8. Plots of experimental (M_n(SEC)) and theoretical (M_n(Theo)) molecular weight vs conversion for polymerization of P(MMA-*co*-PEGMA) (% PEGMA = 10, 18, 24, 30, and 40 mol % PEGMA) in DPE at 25 wt %. $[TSC]_0$:$[Cu(dNBpy)_2Br]_0$ = 1:1 at 70 °C.

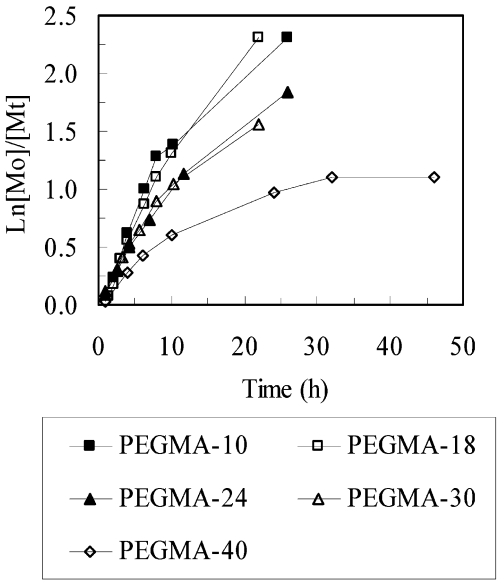

Figure 9. Conversion profiles for polymerization of P(MMA-*co*-PEGMA) (% PEGMA = 10, 18, 24, 30, and 40 mol % PEGMA) in DPE using conditions of Figure 9.

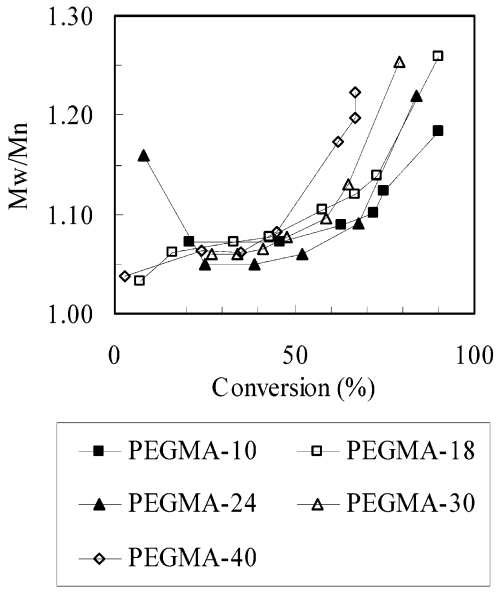

Figure 10. Polydispersity profiles for polymerization of P(MMA-*co*-PEGMA) (% PEGMA = 10, 18, 24, 30, and 40 mol % PEGMA) in DPE using conditions of Figure 9.

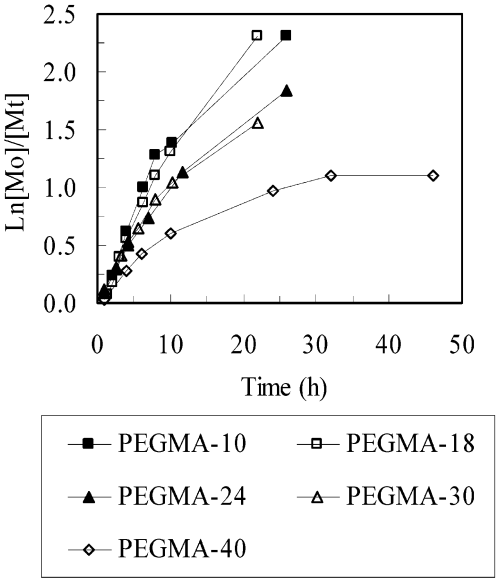

Figure 11. Kinetic profiles for polymerization of P(MMA-*co*-PEGMA) (% PEGMA = 10, 18, 24, 30, and 40 mol % PEGMA) in DPE using conditions of Figure 9.

weights with conversion as expected in an ATRP reaction.

Because of the poor polydispersity observed in the ATRP of P(MMA-*co*-PEGMA) in CXL, further copolymerizations containing 10, 18, 24, 30, and 40 mol % (i.e., 32, 49, 57, 64, and 74 wt %) PEGMA in the feed were conducted in DPE. The copolymer molecular weights increased linearly with conversion and are in good agreement with the theoretical molecular weight (solid line in Figure 8). Increasing the PEGMA content of the comonomer feed from 10 to 40 mol % led to loss of control in the ATRP reaction. This trend is apparent from lower conversion at reaction end (Figure 9), higher polydispersities at a given conversion (Figure 10), and greater curvature in the kinetic plots (Figure 11) with increasing amounts of PEGMA. The increasing curvature in the kinetic plots suggests diminishing radical concentrations, indicating irreversible termination by either coupling or disproportionation of polymeric radicals. The SEC chromatograms in all copolymerizations were bimodal beyond ~30% conversion to polymer with a small high molecular weight peak comprising a quarter of the product (at reaction end) in the copolymerization containing 10 mol % PEGMA and about a third in other cases. This indicates that loss of radical concentration was predominantly due to radical−radical coupling. PEGMA copolymers are known to yield crosslinked gels in conventional free radical polymerizations.[26] The authors attributed the observed crosslinking to relatively high (of the order of 10^{-3}−10^{-4}) chain transfer constants of the oxyethylene units in PEG and PEG derivatives in the polymerization of methacrylates,[35] acrylonitrile,[36] and vinyl acetate.[37] It is probable that the presence of PEG chains in PEGMA

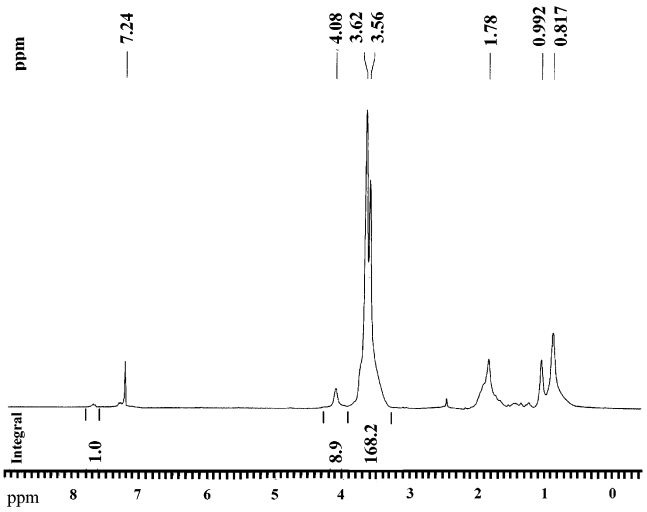

Figure 12. ^{1}H NMR spectrum of P(MMA-*co*-PEGMA) copolymer (in $CDCl_3$) containing 18 mol % PEGMA.

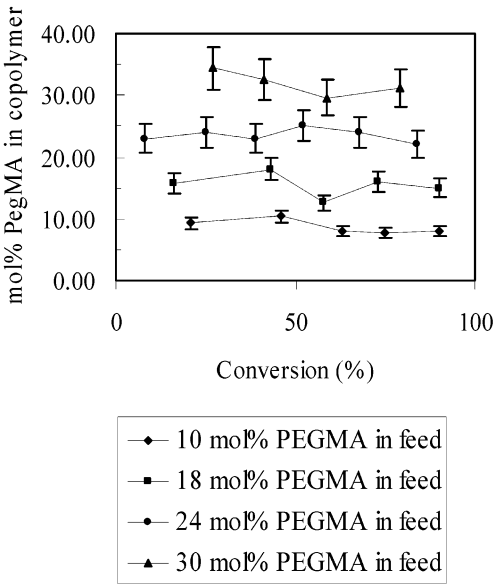

Figure 13. Evolution of PEGMA content in P(MMA-*co*-PEGMA) copolymer with conversion as determined by ^{1}H NMR spectroscopy.

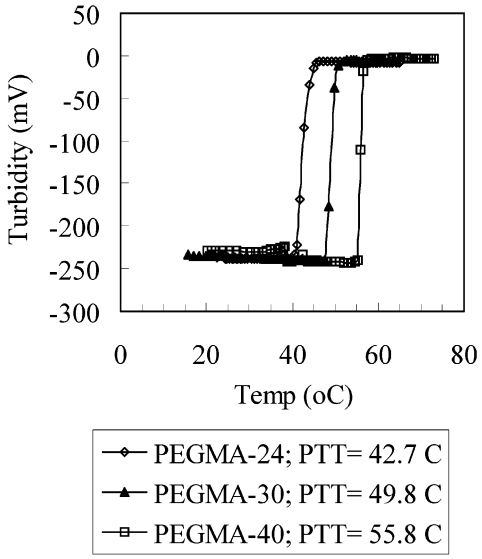

Figure 14. Turbidity vs temperature curves of 1 wt % aqueous solutions of water-soluble P(MMA-*co*-PEGMA) containing 24, 30, and 40 mol % PEGMA showing the phase transition temperatures (42.7, 49.8, and 55.8 °C, respectively) of the copolymers (as determined by location of the point of inflection).

macromonomer and in the forming copolymers causes chain transfer to polymer. This would lead to chain branching and to cross-linking via radical coupling. In ATRP polymerizations, we believe the carbon radicals on the pendant PEG moieties (formed via chain transfer to polymer) as well as methacrylate radicals on chain branches arising thereof are reversibly terminated by atom transfer reaction with the ATRP catalyst, thereby maintaining low radical concentrations characteristic of ATRP (of the order of 10^{-9}–10^{-10} as apposed to 10^{-5}–10^{-7} in conventional free radical polymerization). Hence, the extent of radical–radical coupling reactions is significantly lower in ATRP, leading to hindered cross-linking and network formation. This explains the absence of gel formation during polymerization and the improved shelf life of ATRP polymers, indicating that ATRP is a better means of preparing soluble polymers of poly(ethylene oxide)-based macromonomers.

Copolymer Composition and Microstructure. The composition of P(MMA-*co*-PEGMA) copolymers should reflect the comonomer feed ratio at quantitative conversion. However, the copolymer may be richer in the more reactive monomer in the early stages of the polymerization. Furthermore, since every polymer chain remains alive throughout an ATRP reaction, preferential incorporation of one monomer would yield gradient copolymers. In general, macromonomers are believed to have lower reactivity than the corresponding low molecular weight monomers due to the low concentration of polymerizable groups in the system as well as possible steric hindrance during monomer addition to the growing polymer chain. The composition of P(MMA-*co*-PEGMA) copolymers was monitored by ^{1}H NMR (Figure 12). The methoxy protons of methyl methacrylate monomer (δCH_3O = 3.58 ppm) overlap with all the methylene protons of the pendant PEG chain in the PEGMA monomer (δCH_2O = 3.61 ppm), except the methylene protons next to the ester functionality (δCH_2-OCO = 4.09 ppm). Using an average pendant PEG chain length of 7 ethylene oxide units, the contribution of the methylene protons of the pendant PEG chain to the overlapped peaks at 3.58 and 3.61 ppm was determined by multiplying the area under of the peak at 4.09 ppm by 13. This allowed determination of the ratio of MMA to PEGMA in the copolymers. Figure 13 gives the evolution of copolymer composition with conversion. The copolymer composition reflected the comonomer feed ratio throughout the polymerization, indicating no preferential incorporation of MMA over the PEGMA macromonomer. Thus, the copolymers prepared are random copolymers rather than gradient copolymers.

Temperature-Induced Phase Transitions of Aqueous Homopolymer and Copolymer Solutions. P(PEGMA) and P(PEGMA-*co*-MMA) are polymers comprised of a hydrophobic methacrylate backbone and hydrophilic poly(ethylene glycol) pendant chains. The homopolymer and copolymers containing 57 wt % and above PEGMA are water-soluble (Table 3). The aqueous copolymer solutions exhibit phase transition temperatures that increased with increasing PEGMA content of the copolymer (Figure 14). The water solubility of the copolymers is based on hydrogen-bonding interactions of the pendant PEG chains with water molecules.

Increasing the temperature is expected to induce entropy favored desolvation of the PEG chains causing the inter- and intramolecular polymer−polymer interactions to dominate, thereby leading to polymer precipitation. Since polymer−solvent interactions are favored with increasing PEGMA content in the copolymers, the phase transition temperature increases with PEGMA content as observed.

Conclusion

The atom transfer radical polymerization of macromonomer PEGMA was developed in organic solvents using toluenesulfonyl halide initiator and Cu(I)Br/alkylbipyridine-based catalyst. Commercially available PEGMA was analyzed by LC-MS and purified using a solvent extraction technique that largely removed crosslinking dimethacrylate impurities as well as nonfunctional poly(ethylene glycol). The polymerization rates of PEGMA macromonomer were comparable to those of methyl methacrylate; however, conversions to polymer at reaction end remained low (50−60%). The ATRP reaction failed in polar *n*-butyl acetate. The failure is attributed to very high initial radical concentration (efficient initiation) coupled with slow deactivation which leads to irreversible radical−radical termination and the consequent irreversible buildup of Cu(II) catalytic species as evidenced from the color of the reaction mixture. In less polar diphenyl ether, conversion to polymer was low (∼30%); however, the product polymer exhibited low polydispersity and a monomodal molecular weight distribution, indicating that the polymerization was controlled. We attribute the low conversion to irreversible termination of polymeric radicals via coupling and/or disproportionation. In even less polar xylene, a more favorable activator/deactivator concentration led to more controlled reaction in the early stages of the polymerization. However, the product polymer exhibited a bimodal molecular weight distribution. We propose this is caused by microphase separation of PEGMA in nonpolar xylene, with the equilibrium concentration of Cu(I)/Cu(II) catalyst species within these polymer-rich domains favoring higher radical concentrations and faster polymerization rates. This caused the observed exponential increase in polymer molecular weight and broadening polydispersity in the latter stages of the polymerization. Polymerization in hydrogen-bonding solvents, ethanol and cyclohexanol, yielded narrow disperse polymers of controlled molecular weight that exhibited monomodal molecular weight distributions. The better ATRP control and higher conversion to polymer in these solvent was attributed to higher activator concentration coupled with a fast dynamic Cu(I)/Cu(II) equilibrium.

The ATRP copolymerizations yielded best results in diphenyl ether. Copolymers containing greater than 57 mol % PEGMA were water-soluble. The water-soluble copolymers exhibited sharp phase transition temperatures which increased with increasing PEGMA content as expected. Conventional free radical copolymerizations of PEGMA with hydrophobic monomers are known to yield gels unless chain transfer agents are used. Also, such materials are known to cross-link and become insoluble gels unless stored in solution.[26] Gel formation during polymerization has been attributed to chain transfer to polymer (or monomer) via its PEG moieties. In ATRP polymerizations, we believe the carbon radicals on the pendant PEG moieties (formed via chain transfer to polymer) as well as methacrylate radicals on chain branches arising thereof are reversibly terminated by atom transfer reaction with the ATRP catalyst, thereby maintaining low radical concentrations characteristic of ATRP (on the order of 10^{-9}−10^{-10} as opposed to 10^{-5}−10^{-7} in conventional free radical polymerization). Hence, the extent of radical−radical coupling reactions is significantly lower in ATRP, leading to hindered crosslinking and network formation. This explains the absence of gel formation during polymerization and the improved shelf life of ATRP polymers, indicating that ATRP is a better means of preparing soluble polymers of poly(ethylene oxide)-based macromonomers.

Experimental Section

Materials. Toluenesulfonyl chloride (99+%) and 4,4′-dinonyl-2,2′-dipyridyl (97%), diphenyl ether (99%), cyclohexanol (99%), and *p*-xylene (99%) were purchased from Aldrich and used as received. Poly(ethylene glycol) monomethacrylate (M_n ∼ 360 Da) was purchased from Aldrich (lot # 04023BU) and Polysciences Inc. ($n = 200$; where "*n*" is the molecular weight of the pendant PEG chain; lot # 519486) and purified as described in this paper. Copper(I) bromide (98%, Aldrich) was purified according to a published procedure.[38] Methyl methacrylate (99%) was obtained from Aldrich and passed over a basic alumina column to remove inhibitor. *n*-Butyl acetate (reagent grade), isopropyl ether (reagent grade), neutral alumina, and basic alumina (both Brockman Activity 1, mesh 60−325) were purchased from Fisher Scientific and used as received. Tetrahydrofuran (99%), dichloromethane (reagent grade), hexanes (reagent grade), methanol (HPLC grade), and water (HPLC grade) were purchased from Caledon Laboratories Limited and used as received. Anhydrous ethanol (100%) was purchased from Commercial Alcohols Inc. (Brampton, Ontario). Methylene-d_2 chloride (99.9%) and chloroform-*d* (99.8%) were purchased from Cambridge Isotope Laboratories and used as received.

Isolation of PEG-MA by Solvent Extraction Technique. In a typical PEGMA isolation experiment, 50 mL of PEGMA was dissolved in 200 mL of distilled water and extracted with DPE (2 × 50 mL). The suspension was then separated by centrifugation at 5000 rpm for 5 min. The organic layer (containing the DEG-DMA components) was discarded, and the aqueous phase was extracted with dichloromethane/hexane (3:1) (2 × 250 mL). The suspension was separated as before, the aqueous phase (containing the PEG components) was discarded, and PEG-MA was recovered from the organic phase by rotary evaporation at 40 °C.

ATRP Homopolymerization of PEGMA in Organic Solvent (CXL, ETH, DPE, and BuAc, or XYL). CuBr (36.4 mg, 0.25 mmol), dNBpy (204.4 mg, 0.5 mmol), PEGMA (3206 mg, 7−8 mmol), and solvent (9621 mg) were placed in a round-bottomed flask in a nitrogen-filled glovebag and closed with a septum. TSC (47.7 mg, 0.25 mmol) was dissolved in a 1 g portion of either solvent or monomer in a vial equipped with a septum inside a nitrogen-filled glovebag. The monomer and catalyst solution was degassed in a stream of argon for 30 min and then transferred to an oil bath at 70 °C. The initiator solution was introduced in one aliquot via a syringe that had been previously degassed with a stream of argon for 3 min. Samples (1 mL) were drawn periodically via a previously degassed syringe for gel permeation chromatography (GPC) and conversion measurements. GPC samples (0.2 mL) were prepared by diluting with THF (1 mL) and passing over a neutral alumina column to remove catalyst. Conversion was determined gravimetrically. This involved dilution of 0.8 mL samples to 2 mL with THF, followed by precipitation in 18−19 mL of isopropyl ether in 20 mL vials; the vials were then centrifuged at 3500 rpm, the supernatant decanted, and the precipitate vacuum-dried (at 40 °C) in the dark to constant weight. The polymerizations typically proceeded to 50−70% conversion.

ATRP Copolymerization in DPE (and CXL). The following is a description of the ATRP synthesis of poly(MMA-*co*-PEGMA) containing 18 mol % PEGMA and is typical of all other copolymerizations. CuBr (72.8 mg, 0.5 mmol), dNBpy (408.8 mg, 1.0 mmol), MMA (2000 mg, 20 mmol), PEGMA (2851 mg, 7 mmol), and solvent (17 533 mg) were placed in a round-bottomed flask in a nitrogen-filled glovebag and closed with a septum. TSC (95.3 mg, 0.5 mmol) was dissolved in MMA (1000 mg, 10 mmol) in a vial equipped with a septum inside a nitrogen-filled glovebag. The monomer(s) and catalyst solution was degassed in a stream of argon for 30 min and then transferred to an oil bath at 70 °C. The initiator solution was introduced in one aliquot via a syringe that had been previously degassed with a stream of argon for 3 min. Samples (1 mL) were drawn periodically via a previously degassed syringe for gel permeation chromatography (GPC) and conversion measurements. GPC samples (0.2 mL) were prepared by diluting with THF (1 mL) and passing over a neutral alumina column to remove catalyst. Conversion was determined gravimetrically as described in the homopolymerization section above. The polymerizations typically proceeded to 60−100% conversion.

Measurements. Polymer molecular weight was determined by size exclusion chromatography using a Waters 515 HPLC pump connected to three Waters 5 μm (7.8 × 300 mm) Styragel (HR2, HR3, and HR4) linear columns (exclusion limits 500−20 000, 500−30 000, and 5000−600 000 Da) and a Waters 2414 refractive index detector. The HPLC pump was equipped with a Waters 717 plus autosampler and computer controlled using the Millenium 32 Chromatography Manager. The column and detector temperature were set at 40.0 and 35.0 °C, respectively. Tetrahydrofuran was used as elution solvent (flow rate = 1 mL/min), and narrow disperse linear polystyrene standards were used for calibration.

The identities of the components in poly(ethylene glycol) monomethacrylate macromonomer were confirmed by liquid chromatography mass spectrometry (LCMS). HPLC was performed using a Symmetry Shield reverse phase C-18 column and the same autosampler, HPLC pump, and refractive index detector as for the size exclusion chromatography (described above). HPLC parameters were as follows: sample concentration = 3 wt %; mobile phase: methanol/water = 1:1; injection volume = 30 μL; flow rate = 0.5 mL/min; column temperature (°C)/RI detector temperature (°C)/run time (min) = 35/30/150. Liquid chromatography mass spectrometry (LCMS) was performed using an HPLC coupled to a electrospray mass spectrometer (ESMS). Positive ion electrospray mass spectrometry was performed using a triple quadrapole Micromass Ultima instrument.

The phase transition temperatures of the amphiphilic copolymer solutions were measured using the cloud point method. An automatic PC-Titrator (Mandel) equipped with a temperature probe and a photometer incorporating a 1 cm path length fiber-optics probe (GT-6LD, Mitsubishi) was used to trace the phase transition by monitoring the transmittance of a white light beam. The turbidity of solution was recorded as photoinduced voltage, where a reading of about −220 mV corresponded to a transparent solution below the cloud point and a reading close to 0 mV for the system above the cloud point. The phase transition temperature was defined as the inflection point of the mV vs temperature curve, as determined by the maximum in the first-order derivative. The concentration of the polymer solutions was 1.0 wt %, and the heating rate was 1.0 °C min^{-1}.

The ^{1}H NMR spectra were recorded in CD_2Cl_2 or $CDCl_3$ at 300 MHz on a Bruker AV-300 Instrument.

Acknowledgment. We acknowledge NSERC and 3M Canada for funding this research and Dr. Nicholas Burke for valuable suggestions.

References and Notes

(1) Wang, J.-S.; Matyjaszewski, K. *J. Am. Chem. Soc.* **1995**, *117*, 5614.
(2) Kato, M.; Kamigaito, M.; Sawamoto, M.; Higashimura, T. *Macromolecules* **1995**, *28*, 1721.
(3) Matyjaszewski, K.; Xia, J. *Chem. Rev.* **2001**, *101*, 2921−2990.
(4) Kamigaito, M.; Ando, T.; Sawamoto, M. *Chem. Rev.* **2001**, *101*, 3689−3745.
(5) Prucker, O.; Rühe, J. *Macromolecules* **1998**, *31*, 592−601.
(6) Prucker, O.; Rühe, J. *Macromolecules* **1998**, *31*, 602−613.
(7) Ejaz, M.; Ohno, K.; Tsujii, Y.; Fukuda, T. *Macromolecules* **2000**, *33*, 2870−2874.
(8) Von Werne, T. A.; Germack, D. S.; Hagberg, E. C.; Sheares, V. V.; Hawker, C. J.; Carter, K. R. *J. Am. Chem. Soc.* **2003**, *125*, 3831−3838.
(9) Chen, X.; Randall, D. P.; Perruchot, C.; Watts, J. F.; Patten, T. E.; Von Werne, T. A.; Armes, S. P. *J. Colloid Interface Sci.* **2003**, *257*, 56−64.
(10) Holmberg, S.; Holmlund, P.; Wilén, C.-E.; Kallio, T.; Sundholm, G.; Sundholm, F. *J. Polym. Sci., Part A: Polym. Chem.* **2002**, *40*, 591−600.
(11) Pelton, R. H. *Adv. Colloid Interface Sci.* **2000**, *85*, 1−33.
(12) Jeong, B.; Kim, S. W.; Bae, Y. H. *Adv. Drug Delivery Rev.* **2002**, *54*, 37−51.
(13) Kost, J.; Langer, R. *Adv. Drug Delivery Rev.* **2001**, *46*, 125−148.
(14) Mathur, A. M.; Drescher, B.; Scranton, A. B.; Klier, J. *Nature (London)* **1998**, *392*, 367−370.
(15) Saunders, B. R.; Koh, A. Y. C. *Chem. Commun.* **2000**, 2461−2462.
(16) Kanazawa, H.; Matsushima, Y.; Okano, T. *Adv. Chromatogr.* **2001**, *41*, 311.
(17) Ista, L. K.; Perez-Luna, V. H.; López, G. P. *Appl. Environ. Microbiol.* **1999**, *65*, 1603.
(18) Hoffman, A. S.; Afrassiabi, A.; Dong, L. C. *J. Controlled Release* **1986**, *4*, 213−222.
(19) Okahata, Y.; Lim, H. J.; Nakamura, G.; Hachiya, S. *J. Am. Chem. Soc.* **1983**, *150*, 4855.
(20) Kidchob, T.; Kimura, S.; Imanishi, Y. *J. Chem. Soc., Perkin Trans. 2* **1997**, 2195−2199.
(21) Peng, T.; Cheng, Y.-L. *Polymer* **2001**, *42*, 2091−2100.
(22) Neugebauer, D.; Zhang, Y.; Pakula, T.; Sheiko, S. S.; Matyjaszewski, K. *Macromolecules* **2003**, *36*, 6746−6755.
(23) Neugebauer, D.; Zhang, Y.; Pakula, T.; Matyjaszewski, K. *Polymer* **2003**, *44*, 6863−6871.
(24) Han, S.; Hagiwara, M.; Ishizone, T. *Macromolecules* **2003**, *36*, 8312−8319.
(25) Ishizone, T.; Han, S.; Okuyama, S.; Nakahama, S. *Macromolecules* **2003**, *36*, 42−49.
(26) Bo, G.; Wesslén, B.; Wesslén, K. B. *J. Polym. Sci., Part A: Polym. Chem.* **1992**, *30*, 1799−1808.
(27) Ali, M. M.; Stöver, H. D. H. *Macromolecules* **2003**, *36*, 1793−1801.
(28) Klier, J.; Scranton, A. B.; Peppas, N. A. *Macromolecules* **1990**, *23*, 4944−4949.
(29) Percec, V.; Barboiu, B.; Kin, H.-J. *J. Am. Chem. Soc.* **1998**, *120*, 305−316.
(30) Matyjaszewski, K.; Nanda, A. J. *Macromolecules* **2003**, *36*, 599−604.
(31) Destarac, M.; Alric, J.; Boutevin, B. *Macromol. Rapid Commun.* **2000**, *21*, 1337−1341.
(32) Chambard, G.; Klumperman, B.; German, A. L. *Macromolecules* **2000**, *33*, 4417−4421.
(33) Ali, M. M.; Stöver, H. D. H. In *Advances in Controlled/Living Radical Polymerization*; Matyjaszewski, K., Ed.; *ACS Symp. Ser.* **2003,** *854*, 299−315.
(34) Haddleton, D. M.; Perrier, S.; Bon, S. A. F. *Macromolecules* **2000**, *33*, 8246−8251.
(35) Nandi, U. S.; Kumar, S.; Bhaduri, G. C. *Indian J. Chem.* **1981**, *20A*, 759.
(36) Schneider, A.; Fritzsche, P. *Acta Polym.* **1979**, *30*, 270.
(37) Okamura, S.; Katagiri, K.; Motoyama, T. *J. Polym. Sci.* **1960**, *43*, 509.
(38) Keller, R. N.; Wycoff, H. D. *Inorg. Synth.* **1946**, *2*, 1.

MA030485M